Developmental Biology 366 (2012) 204–217

Contents lists available at SciVerse ScienceDirect

Developmental Biology

journal homepage: www.elsevier.com/locate/developmentalbiology

Developmental changes in expression, subcellular distribution, and function of *Drosophila* N-cadherin, guided by a cell-intrinsic program during neuronal differentiation

Mitsuhiko Kurusu [a,*], Takeo Katsuki [b], Kai Zinn [c], Emiko Suzuki [a]

[a] *Structural Biology Center, National Institute of Genetics and Department of Genetics, The Graduate University for Advanced Studies, Mishima 411-8540, Japan*
[b] *Kavli Institute for Brain and Mind, University of California, San Diego, La Jolla, CA 92093, USA*
[c] *Broad Center, Division of Biology, California Institute of Technology, Pasadena, CA 91125, USA*

ARTICLE INFO

Article history:
Received 14 December 2011
Received in revised form
2 April 2012
Accepted 3 April 2012
Available online 19 April 2012

Keywords:
Axon guidance
Synaptogenesis
Mushroom body
Neuromuscular junction
N-cadherin
Drosophila

ABSTRACT

Cell adhesion molecules (CAMs) perform numerous functions during neural development. An individual CAM can play different roles during each stage of neuronal differentiation; however, little is known about how such functional switching is accomplished. Here we show that *Drosophila* N-cadherin (CadN) is required at multiple developmental stages within the same neuronal population and that its sub-cellular expression pattern changes between the different stages. During development of mushroom body neurons and motoneurons, CadN is expressed at high levels on growing axons, whereas expression becomes downregulated and restricted to synaptic sites in mature neurons. Phenotypic analysis of *CadN* mutants reveals that developing axons require CadN for axon guidance and fasciculation, whereas mature neurons for terminal growth and receptor clustering. Furthermore, we demonstrate that CadN downregulation can be achieved in cultured neurons without synaptic contact with other cells. Neuronal silencing experiments using $Kir_{2.1}$ indicate that neuronal excitability is also dispensable for CadN downregulation *in vivo*. Interestingly, downregulation of CadN can be prematurely induced by ectopic expression of a nonselective cation channel, dTRPA1, in developing neurons. Together, we suggest that switching of CadN expression during neuronal differentiation involves regulated cation influx within neurons.

Introduction

Cell adhesion molecules (CAMs) and receptor proteins control various developmental processes during neural circuit formation. Some of the CAMs and receptors that regulate axon guidance are also required for normal synaptogenesis and synaptic plasticity. The distinct requirements for CAMs and receptors in these different developmental processes suggest that the expression and function of these proteins are coordinated with neuronal differentiation. The mechanisms involved in such functional switching are poorly understood.

Classic cadherins are one such class of proteins that have distinct roles in developing and mature neurons. They are an evolutionarily conserved family of calcium-dependent homophilic CAMs. Among the classic cadherins, N-cadherin has been most extensively studied. Vertebrate N-cadherin is widely expressed in neural tissues during embryonic development as well as in the mature nervous system (Suzuki and Takeichi, 2008). Neurodevelopmental studies in a variety of vertebrate and invertebrate models, including chick, rat, zebrafish, *Drosophila*, and *C. elegans*, have implicated N-cadherin in axonal outgrowth, fasciculation, target selection, and dendritic arborization during early stages of developments. Moreover, N-cadherin regulates neurite extension in cultured neurons (Matsunaga et al., 1988; Doherty et al., 1991, 1992). *In vivo*, it controls axon guidance and targeting of retinal, olfactory, thalamocortical, and motor axons (Inoue and Sanes, 1997; Iwai et al., 1997; Lee et al., 2001; Broadbent and Pettitt, 2002; Masai et al., 2003; Poskanzer et al., 2003; Hummel and Zipursky, 2004; Zhu and Luo, 2004). During later stages of development, N-cadherin expression often becomes restricted to presynaptic transmitter release zones and to postsynaptic densities (Yamagata et al., 1995; Fannon and Colman, 1996; Uchida et al., 1996; Benson and Tanaka, 1998; Elste and Benson, 2006). siRNA knockdown of N-cadherin attenuated the growth of dendritic spines on cultured hippocampal neurons, suggesting that postsynaptic N-cadherin is required for synapse formation (Saglietti et al., 2007). Moreover, N-cadherin contributes to the stabilization of glutamate-receptor (GluR) clustering (Coussen et al., 2002; Nuriya and Huganir, 2006; Saglietti et al., 2007), as well

* Corresponding author. Fax: +81 55 981 6842.
E-mail address: mkurusu@lab.nig.ac.jp (M. Kurusu).

0012-1606/$ - see front matter © 2012 Elsevier Inc. All rights reserved.
http://dx.doi.org/10.1016/j.ydbio.2012.04.006

as to activity-dependent synaptic plasticity (Tang et al., 1998; Bozdagi et al., 2000; Jüngling et al., 2006). *Drosophila* mutant analysis also revealed that its N-cadherin homolog, CadN, participates in organizing the ultrastructure of the synapses between photoreceptor cells and postsynaptic L-cells (Iwai et al., 2002).

These results indicate that N-cadherin is required for axonal growth, dendritic morphogenesis, and synaptogenesis during development, as well as for synaptic transmission and synaptic plasticity in the mature nervous systems. However, in most cases it has not been shown that N-cadherin has multiple functions within the same neuron. The only *in vivo* exception to this is for *Drosophila* photoreceptor cells, where CadN is required for both axon targeting and creation of a normal synaptic ultrastructure, but a detailed analysis of the dynamics of CadN expression in these cells during neuronal maturation has not been performed (Lee et al., 2001; Iwai et al., 2002).

In this paper, we examined whether there are distinct requirements for *Drosophila* CadN function during axonal outgrowth and synaptogenesis within defined neuronal populations *in vivo*. We focused on two sets of neurons, mushroom body (MB) neurons and motoneurons, each of which has distinct advantages for morphological analysis. The MB, a brain center for olfactory associative memory, is composed of thousands of neurons that are continuously derived from MB-specific neuroblasts until the late pupal stage. MBs therefore provide an opportunity to observe newly born neurons and mature neurons simultaneously, although the neurites are too small for fine structural analysis under light microscopy. On the other hand, motoneuronal networks innervating larval body wall muscles display simple trajectories and have large glutamatergic neuromuscular junctions (NMJs). The neuromuscular networks are assembled by the end of embryogenesis and subsequent growth of NMJs during larval life is regulated by neuronal activity. The predictable developmental pattern of embryonic motoneurons as well as the stereotyped cytoarchitecture of the NMJ allow for high-resolution imaging and quantification of axonal projection patterns and NMJ structure with single-synapse resolution.

Here we demonstrate that CadN expression is similarly altered during neuronal differentiation in both circuits. In developing neurons, high levels of CadN are distributed diffusely along axons. Expression is downregulated as neurons mature and concentrated to areas adjacent to presynaptic and postsynaptic sites. Mutant analyses confirm that CadN is necessary for axon guidance and synaptogenesis in both circuits. Low-density neuronal culture experiments suggest that the developmental switch in the CadN expression pattern is triggered by a cell-autonomous program independent of synaptic contacts. We also show that activation of an ectopically expressed temperature-sensitive cation channel, dTRPA1, in developing MB neurons can prematurely shift CadN expression to the mature pattern, implying that cation influx controls the switching process.

Materials and methods

Drosophila stocks

Oregon R, w^{1118}, OK107 (Bloomington Stock Center (BSC)), 201Y (BSC), *elav-Gal4* (II, BSC), UAS-*mCD8GFP* (II, BSC), UAS-*mCD8GFP* (III, BSC), $CadN^{18A\ stop}$ (Nern et al., 2005), $CadN^{M12}$ (Iwai et al., 1997), $CadN^{M19}$ (Iwai et al., 1997), $CadN^{\Delta 14}$ (Prakash et al., 2005), $CadN2^{\Delta 7}$ (Prakash et al., 2005), UAS-*CadN* (X) (Iwai et al., 1997), UAS-*dTRPA1* (II, BSC), UAS-$Kir_{2.1}$ (Baines et al., 2001), $CadN^{M19}$ FRT40A, and $CadN^{\Delta 14}$ FRT40A were used.

Immunostaining

For MB preparations, the dissected brains were fixed with 4% paraformaldehyde for 30 min at room temperature. Washing was done with 0.3% Triton X-100 in PBS. Blocking was done in PBS containing 0.3% Triton X-100, 0.1% BSA, and 5% normal goat serum. Incubation with primary and secondary antibodies was done overnight at 4 °C. Labeled samples were mounted with anti-fade Vectashield medium (Vector Laboratories, Inc.). For NMJ preparations, larvae were dissected in HL3 saline (+1.5 mM Ca^{2+}) and the fillets were fixed with 3.7% formaldehyde solution (Wako) for 30 min at room temperature. Subsequent immunohistochemical processing was done as described for MB preparations. For staining with anti-GluRIIA, the dissection was done in HL3 saline (+1.5 mM Ca^{2+}) and the fillets were fixed for 3 min with Bouin's solution (Sigma-Aldrich). Fixed samples were then processed as above. For staining cultured neurons, cells were fixed with 3.7% formaldehyde solution (Wako) for 20 min at room temperature and stained using the protocol described for MB tissue. Confocal images were captured with a Zeiss LSM510 microscope.

The following antibodies were used: goat FITC-conjugated anti-horseradish peroxidase (HRP) (1:200; Jackson ImmunoResearch), rat anti-CadN (1:200; EX-#8; Iwai et al., 1997), mouse anti-SYN (1:10; 3C11; DSHB), mouse anti-BRP (1:100; nc82; DSHB), mouse anti-FAS II (1:5; 1D4; DSHB), mouse anti-GluRIIA (1:50; 8B4D2; DSHB), mouse anti-NRT (1:10; BP106; DSHB), rat anti-mCD8α (1:100; Invitrogen), and FITC-, DyLyght488-, Cy3-, DyLyght649-, and Cy5-conjugated secondary antibodies (1:400; Jackson ImmunoResearch). Alexa Fluor-conjugated phalloidin was diluted 1:50 (Invitrogen).

MARCM system

The following genotypes were examined for loss-of-function analysis: hs-*flp* UAS-*mCD8GFP*; $CadN^{M19}$ FRT40A/tub-*Gal80* FRT40A; OK107/+ and hs-*flp* UAS-*mCD8GFP*; $CadN^{\Delta 14}$ FRT40A/tub-*Gal80* FRT40A; OK107/+. The following genotype was examined for gain-of-function analysis: hs-*flp* UAS-*mCD8GFP*/UAS-*CadN*; FRT40A/tub-*Gal80* FRT40A; OK107/+. Eggs were collected within a 2-h window on standard fly food at 25 °C. For marking MB clones generated at first instar stage, a 60-min heat shock (37 °C) was applied at 27 h after the start of egg collection. Clones were examined at the wandering larval stage. For marking MB clones generated at the early third instar stage, a 60-min heat shock (37 °C) was applied at 75 h after the start of egg collection. Clones were examined at the wandering larval stage. For marking MB clones generated at mid-pupal stage, eggs were collected within a 4-h window. A 60-min heat shock at 37 °C was applied at 172 h after the start of egg collection. Clones were examined at the adult stage.

Cell culture

Primary cell cultures of *Drosophila* embryonic neurons were prepared as described previously (Katsuki et al., 2009). To detect neurons, *elav*-Gal4 UAS-*mCD8GFP* flies were used. Briefly, neurons before undergoing axogenesis were obtained at embryonic stages 9–11. The dissociated cells were suspended in Schneider's *Drosophila* medium (GIBCO) supplemented with 10% fetal bovine serum, and cultured on glass-bottom dishes (MatTek) coated with 1 mg/ml poly-DL-ornithine (Sigma-Aldrich). Cell density was adjusted to minimize cell–cell contacts. Cultures were kept at 25 °C without additional CO_2 and fixed 6, 12, 18, 24, 30, 36, and 48 h after seeding.

Quantitative analysis

For the quantification of GluR fields, third instar larval fillets of wild type and mutants were stained with anti-GluRIIA, and Type Ib boutons on muscle 4 of A3 segments were captured with identical gain, offset, AOTF, and zoom levels on a Zeiss LSM510

microscope. The captured image stacks were processed with IMARIS 7 (Bitplane) 3D image analysis software. By using the surface wizard, reliable visualization of GluR fields was obtained in wild-type samples, and the mean surface areas of GluR fields were then determined in wild type and mutants. The settings included smooth (0.13 μm), background subtraction (largest sphere diameter, 0.3 μm; threshold, 2.5 μm^2), and seed detection diameters (0.3 μm).

For the quantification of CadN and SYN expression levels in cultured neurons, neurons expressing mCD8GFP were double-stained with anti-CadN and anti-SYN, and confocal images were captured with the identical gain, offset, AOTF, and zoom levels throughout the culture time. Captured images were analyzed semi-automatically using a custom program written in R software (The R Foundation) with the EBImage package. Binary image masks of neurons were created based on mCD8GFP fluorescence and were used to measure immunofluorescence intensities of CadN and SYN. Background subtraction was done by manually selecting a 50 pixel by 50 pixel background area in each image. For statistical processing, outliers detected with the Grubbs' test were excluded from further analysis.

dTRPA1 activation

To express dTRPA1 in the MB and mark those neurons with CD8GFP, the 201Y/+; UAS-*mCD8GFP*/UAS-*dTRPA1* genotype was examined. Eggs were collected within a 3-h window on standard fly food at 18 °C. The embryos were kept at 18 °C until wandering larvae first emerged on the wall. These wandering larvae were examined as controls without dTRPA1 activation. The remaining larvae in the food were shifted to 29 °C for heat-activation of dTRPA1. After 3, 6, or 9 h of dTRPA1 activation at 29 °C, wandering larvae were examined.

Results

CadN expression patterns are developmentally regulated in MB neurons

To explore the role of CadN in developing neurons and mature neurons, we first focused on the larval MB, a bilateral neural structure that receives inputs from the olfactory system (Fig. 1A). In each brain hemisphere, MB neurons are produced by four neuroblasts that continuously proliferate up to the late pupal stage (Ito and Hotta, 1992). MB neurons extend dendrites into a glomerular structure called the calyx (Fig. 1B) that receives inputs from the olfactory projection neurons (PNs). The axons of MB neurons from each lineage fasciculate into a bundle to form the peduncle, a parallel tract that extends ventrally and then splits into two branches, the dorsal and medial lobes (Fig. 1B). The internal organization of the MB axon bundle reflects the temporal order of neuronal birth; axons from sequentially generated later-born neurons project into the core of the peduncle and displace the older core axons to the periphery, establishing a concentric layer arrangement (Kurusu et al., 2002).

We determined CadN expression patterns in the third instar MBs by anti-CadN immunostaining. Here, developing neurons were visualized by lower levels of mCD8GFP expression driven by OK107-GAL4 (OK107 > GFP), and mature neurons by stronger expression of OK107 > GFP (Kurusu et al., 2002). Strong CadN immunoreactivity was detected in the cell bodies of developing MB neurons (Fig. 1C) as well as in the core axons of peduncles and lobes (arrowheads in Fig. 1E and F). In contrast, CadN expression was dramatically downregulated in the cell bodies of mature neurons (Fig. 1C). Downregulation of CadN was also seen in the mature axons located at the periphery of the peduncles and lobes (Fig. 1E and F). Moreover, CadN signals in the periphery of peduncle were punctate when observed in cross-section (see bracket in Fig. 1E), whereas CadN in the developing neurons was uniformly distributed along the axons (Fig. 1E and F).

Similar to third instar MB axons, core axons in first and second instar larvae intensely expressed CadN, while expression in surrounding mature axons was much weaker (Suppl. Fig. 1A–D). In the adults, all mature MB neurons exhibited reduced expression of CadN (Suppl. Fig. 1E and F). These results illustrate the general expression profile of CadN in *Drosophila* MB neurons; strong expression in developing neurons and weak expression in mature neurons.

CadN is localized to synaptic regions in mature MB dendrites

Although mature neurons showed diminished levels of CadN in their cell bodies and axons, significant levels of CadN signals were detected in the calyx of third instar larvae and adults (Figs. 1D and 2), indicating that CadN is localized to dendrites in mature neurons. To further define CadN localization in the dendrites, we focused on the adult calycal sections at high resolution, and compared localization patterns of CadN with synaptic markers. MB dendritic endings in the calyx form microglomerular structures harboring presynaptic terminals from olfactory PNs, displaying most characteristics of postsynaptic specialization including actin enrichment and postsynaptic regulators (Fig. 2A) (Yasuyama et al., 2002; Leiss et al., 2009). The microglomerulus is observed as a ring-like structure by mCD8GFP expression under OK107-Gal4 (Fig. 2B and C). CadN signals partially overlapped the microglomerular rings with slight penetration into the inner region (Fig. 2B, C, and F), where presynaptic terminals of PNs labeled with anti-Synapsin (SYN) are concentrated (Fig. 2D and F). Postsynaptic localization of CadN was evident from colocalization of CadN and Discs large (DLG), a PSD-95 homolog in *Drosophila* (Fig. 2E). These results suggest that CadN is localized to the MB input synapses.

CadN is required for fasciculation, proper outgrowth, and branching of axons in developing MB neurons

To determine if CadN is required for correct axon guidance during MB development, we analyzed several widely used *CadN* mutants. The CadN locus contains three modules of alternatively spliced exons and encodes 12 isoforms (Ting et al., 2005). $CadN^{18A\ stop}$ contains a nonsense mutation within alternative exon 18a, resulting in the production of variants containing exon 18b (Nern et al., 2005). $CadN^{M12}$ is a hypomorphic mutant that contains an amino acid substitution within the conserved cadherin domain among isoforms (Iwai et al., 1997). $CadN^{M19}$ is a truncation mutant that is thought to be null (Iwai et al., 1997). $CadN^{\Delta 14}$ is a deletion mutant that eliminates *CadN* and its sister gene *CadN2* (Prakash et al., 2005). Because *CadN* null mutants showed embryonic lethality, we first examined two viable trans-heterozygous mutant combinations ($CadN^{M12}/CadN^{\Delta 14}$ and $CadN^{18A\ stop}/CadN^{\Delta 14}$). In these experiments, mature axons in the third instar larval MB were visualized with anti-Fasciclin II (FasII) (Kurusu et al., 2000) and the core axons were visualized by phalloidin staining (Kurusu et al., 2002).

The *CadN* hypomorphic mutant $CadN^{M12}/CadN^{\Delta 14}$ had significant defects in axonal morphology. In 100% (15/15) of wild types, the medial lobes extended toward and terminated near the edge of a midline region (Fig. 3A), while in 64% (9/14) of $CadN^{M12}$ mutants, the medial lobes extended beyond the termination zone to fuse at the midline (star in Fig. 3C). This suggests that CadN is required for stopping medial branching at the midline. Moreover, in 43% (12/48) of the mutant MBs, the dorsal lobes were reduced or entirely absent

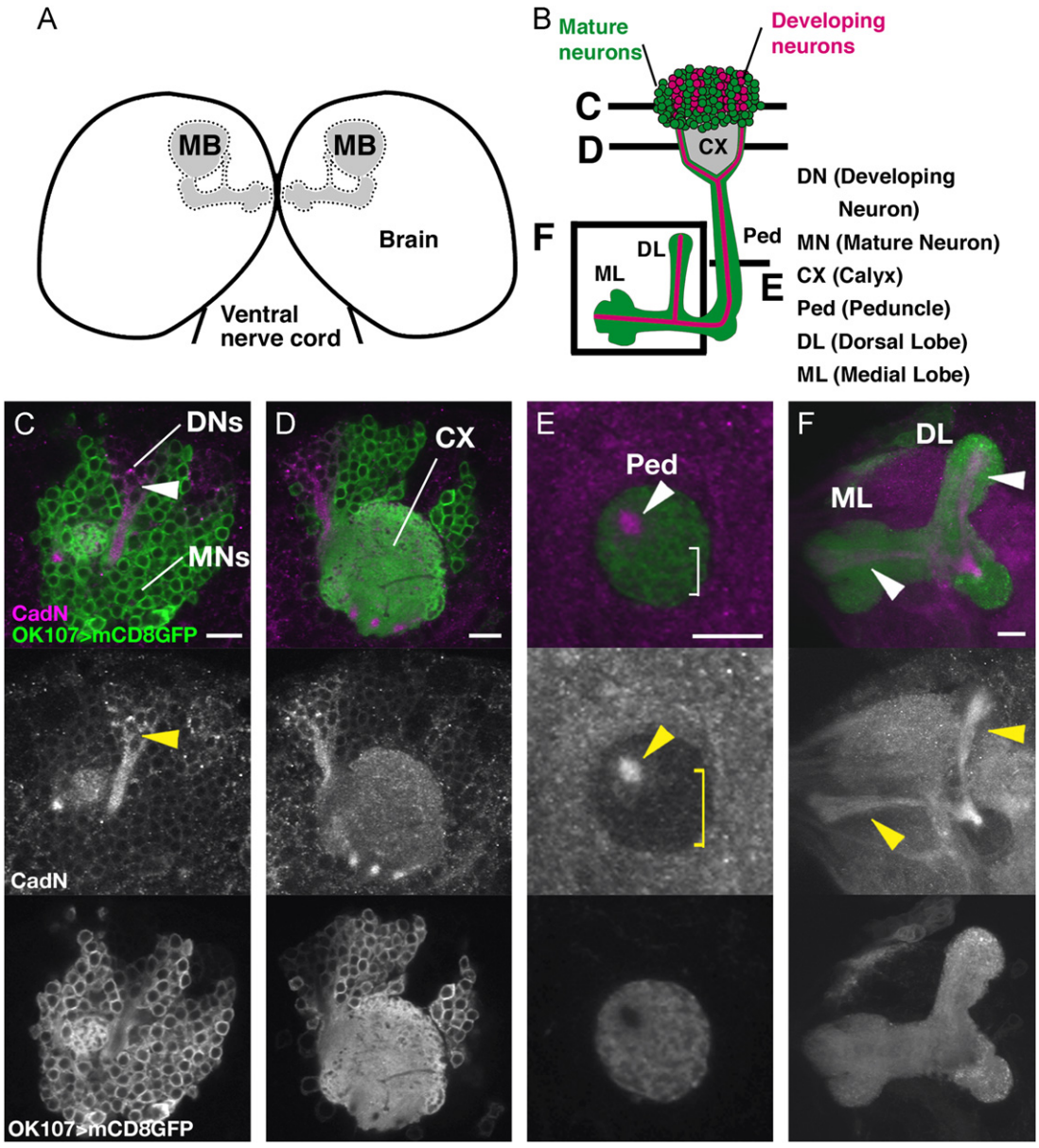

Fig. 1. CadN expression patterns in the third instar larval mushroom body (MB). (A and B) Schematic representation of the larval brain indicating MB position (A) and the larval MB (B). Developing neurons are represented in magenta and mature neurons in green. Focal positions of panels (C–F) are indicated by planes through the MB diagram in (B). (C–F) MBs are visualized with the OK107 > UAS-*mCD8GFP* (green). Anti-CadN (magenta). In each panel, the arrowheads indicate regions showing strong expression of CadN. (C–E) Single sections through a MB cell body cluster (C), calyx region (D), and peduncle (E). (F) Z-stack projection of lobes. Scale bars: 10 μm.

(Fig. 3C). Peduncle cross-sections revealed that 57% (16/28) of mutant MBs had smaller core bundles than wild types ($n=30$) (Fig. 3B and D) even though neurons were produced at the normal rate (Suppl. Fig. 2). The small size in the mutant core bundles probably reflects reduced fasciculation of developing axons as they extend into the peduncle. In contrast to the hypomorphic mutants, the MB defects observed in the $CadN^{18A\ stop}/CadN^{\Delta 14}$ mutant were mild (ML fusion, 1/14; branch defect, 4/24; fasciculation defect, 2/28) (Fig. 3E and F), indicating that CadN variants including alternative exon 18b can partially rescue the normal MB axonal morphology in the presence of the $CadN^{\Delta 14}$ deletion mutation. Thus, CadN variants containing exon 18b are probably the major isoforms mediating fasciculation and midline termination of developing axons in the medial lobe.

To precisely define the role of CadN in MB development, we examined the null mutants $CadN^{M19}$ and $CadN^{\Delta 14}$ using the mosaic analysis with a repressible cell marker (MARCM) system, which produces inducible null mutant clones with selective GFP-labeling on a heterozygous genetic background (Lee et al., 1999). The clones were induced at the first instar stage and analyzed for their axonal structure at the third instar stage. Both $CadN^{M19}$ and $CadN^{\Delta 14}$ mutant clones exhibited a medial-lobe overextension phenotype (Control, 0/10; $CadN^{M19}$, 8/14; $CadN^{\Delta 14}$, 4/13) (Fig. 3H and data not shown) similar to those seen in whole animals bearing the hypomorphic mutations (Fig. 3C). Mutation of the *CadN2* gene ($CadN2^{\Delta 7}$) did not show any morphological MB defects (Suppl. Fig. 3), indicating that the $CadN^{\Delta 14}$ phenotype is due to loss of CadN. No branching defects were observed in $CadN^{M19}$ and $CadN^{\Delta 14}$ mutant clones, suggesting that the deficits observed in the hypomorphic $CadN^{M12}/CadN^{\Delta 14}$ mutant larvae, with dorsal lobes reduced or absent, may only emerge when all MB axons lack functional CadN or when clone size is larger. These results suggest that CadN is required for proper extension of MB axons.

CadN null mutations caused a mild defasciculation phenotype in addition to the medial lobe fusion phenotype. The core axons

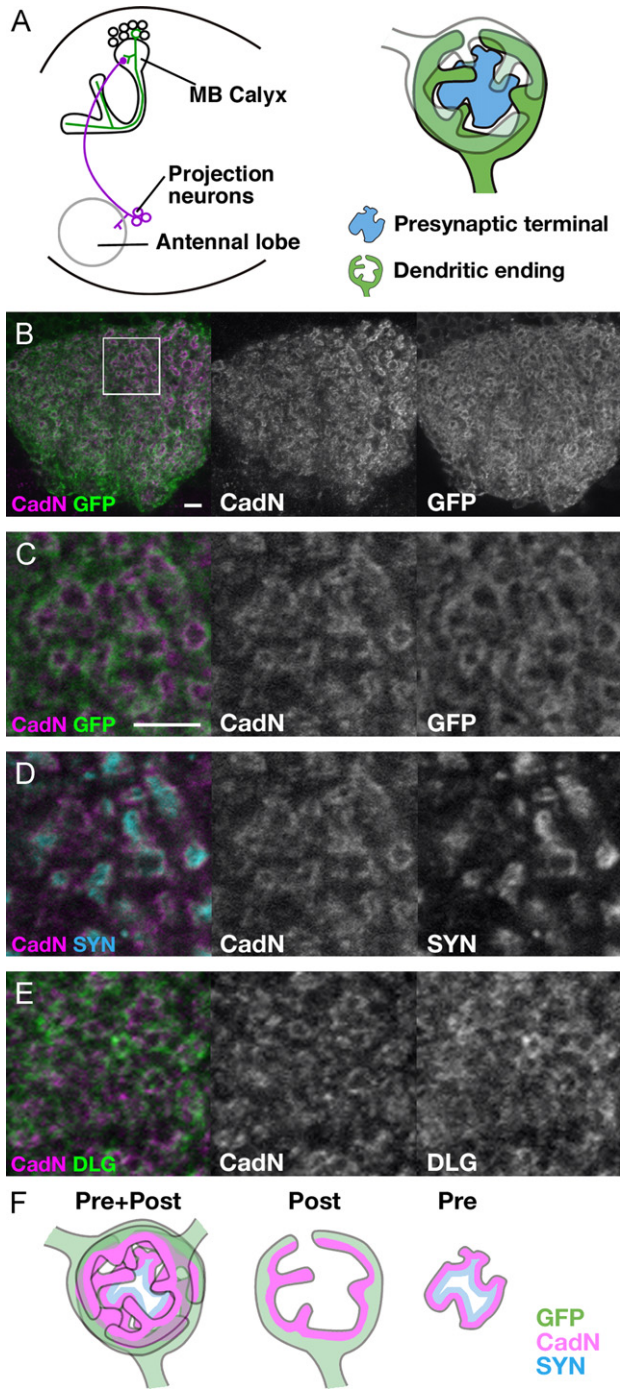

Fig. 2. CadN expression patterns in the adult calycal microglomeruli. (A) Left panel shows the olfactory pathway in the *Drosophila* brain. MB dendritic endings in the calyx receive cholinergic input from olfactory projection neurons. Right panel shows microglomerular organization in the calyx. MB dendritic endings form microglomeruli harboring presynaptic terminals from olfactory PNs. (B) Single section through adult MB calyx expressing mCD8GFP (green) under OK107. Anti-CadN (magenta). Microglomeruli are recognized as ring-like structures. (C and D) High-magnification images corresponding to the inset in (B). OK107 > UAS-*mCD8GFP* (green), anti-CadN (magenta), and anti-SYN (cyan). Single sections. CadN signals straddle the region between the MB dendritic regions and the presynaptic fields of PNs labeled with anti-SYN. (E) A high-magnification image of calycal region labeled with anti-CadN (magenta) and anti-DLG (green). Single section. CadN is colocalized to postsynaptic DLG in ring-like microglomeruli. (F) Schematic representation of microglomerulus showing GFP (green), CadN (magenta), and SYN (blue) expressions. Scale bars: 5 μm in (B); 5 μm in (C), applies also to (D and E).

were examined by dissecting third instar larvae shortly after clone induction. While each wild-type clone formed a single unified fascicle in the core (Fig. 3I), 18% (4/22) of $CadN^{\Delta 14}$ mutant clones produced multiple (> 3) core bundles (Fig. 3J). Although penetrance was lower than the medial-lobe overextension phenotype, it was comparable to defasciculation phenotypes observed in mutants of other axon-guidance molecules (see Discussion). Thus, the null mutation analyses with MARCM revealed that CadN is required for fasciculation of MB axons.

The strong CadN expression observed in developing neurons was markedly downregulated during development and maintained at low levels in mature neurons (Fig. 1), implying that downregulation of CadN in mature neurons is critical for proper MB development. To test this, we overexpressed CadN specifically in mature neurons using 201Y-Gal4, which is expressed only in mature MB neurons at larval stage (Kurusu et al., 2002). CadN overexpression in mature neurons caused severe deficits in axon guidance (reduced medial lobes, 6/13, arrowhead in Fig. 3M; split core bundles, 5/7, arrowheads in Fig. 3N). The defects may be caused by an increased affinity between developing axons and the surrounding layer of mature axons. Thus, downregulation of CadN in mature neurons is likely to be required for proper development of MB axonal structure, possibly by reducing the affinity between developing and mature axons.

CadN affects the elaboration of fine dendritic processes in the MB calyx

Co-labeling MBs with antibodies against CadN and pre- and postsynaptic proteins suggests that mature neurons express CadN near synaptic terminals in calyx dendrites (see Fig. 2). To determine if CadN expression is necessary for proper morphogenesis of synaptic terminals in MBs, we examined development of dendritic terminal structures in wild-type and mutant adults using confocal microscopy. The adult MB contains at least three sets of neurons (γ, α′/β′, and α/β) that differ in birth order and occupied lobes (Lee et al., 1999). We focused on α/β neurons, which are implicated in long-term olfactory memory (Pascual and Preat, 2001), and captured high resolution images of single or two-cell clones induced at mid-pupal stage and dissected in adults. Wild-type clones exhibited several dendritic branches from the main shaft, most of which (77%, 66/96) terminated in characteristic claw-like structures with fine processes (Fig. 4A and indicated with blue arrowheads in Fig. 4B) that form postsynaptic specializations and microglomeruli apposed to presynaptic terminals from olfactory PNs (see Fig. 2A) (Yasuyama et al., 2002; Leiss et al., 2009). In $CadN^{M19}$ null mutant clones, 48% (78/163) of dendritic endings became small with less complex processes (classified as "small" in Fig. 4A and indicated with magenta arrowheads in Fig. 4C) and 13% (20/163) of endings resulted in the complete loss of fine processes (classified as "loss" in Fig. 4A and indicated with green arrowhead in the lower panel of Fig. 4C). These results indicate that CadN is required for the elaboration of the fine dendritic processes.

We also performed CadN overexpression in which CadN was induced at the timing of clone induction. 72% (73/101) of endings showed "loss" defects completely lacking fine processes (Fig. 4A and green arrowheads in Fig. 4D), suggesting that proper elaboration of dendritic fine processes requires an optimal range of CadN expression. However, since CadN was driven by OK107 in this experiment, it remains unclear whether the gain-of-function phenotype in dendrites was due to the effect of continuous CadN overexpression from developing stage through to mature stage, or the effect of CadN overexpression only during the mature stage. To distinguish these possibilities, we induced CadN specifically in mature neurons using 201Y-Gal4, which is expressed only in mature MB neurons at larval stage (Kurusu et al., 2002) and examined whole larval calyx, since there is no Gal4-driver to be expressed specifically in mature neurons at pupal stage. Specific induction of CadN in mature neurons resulted in loss of microglomerular structures and reduced staining of synaptic

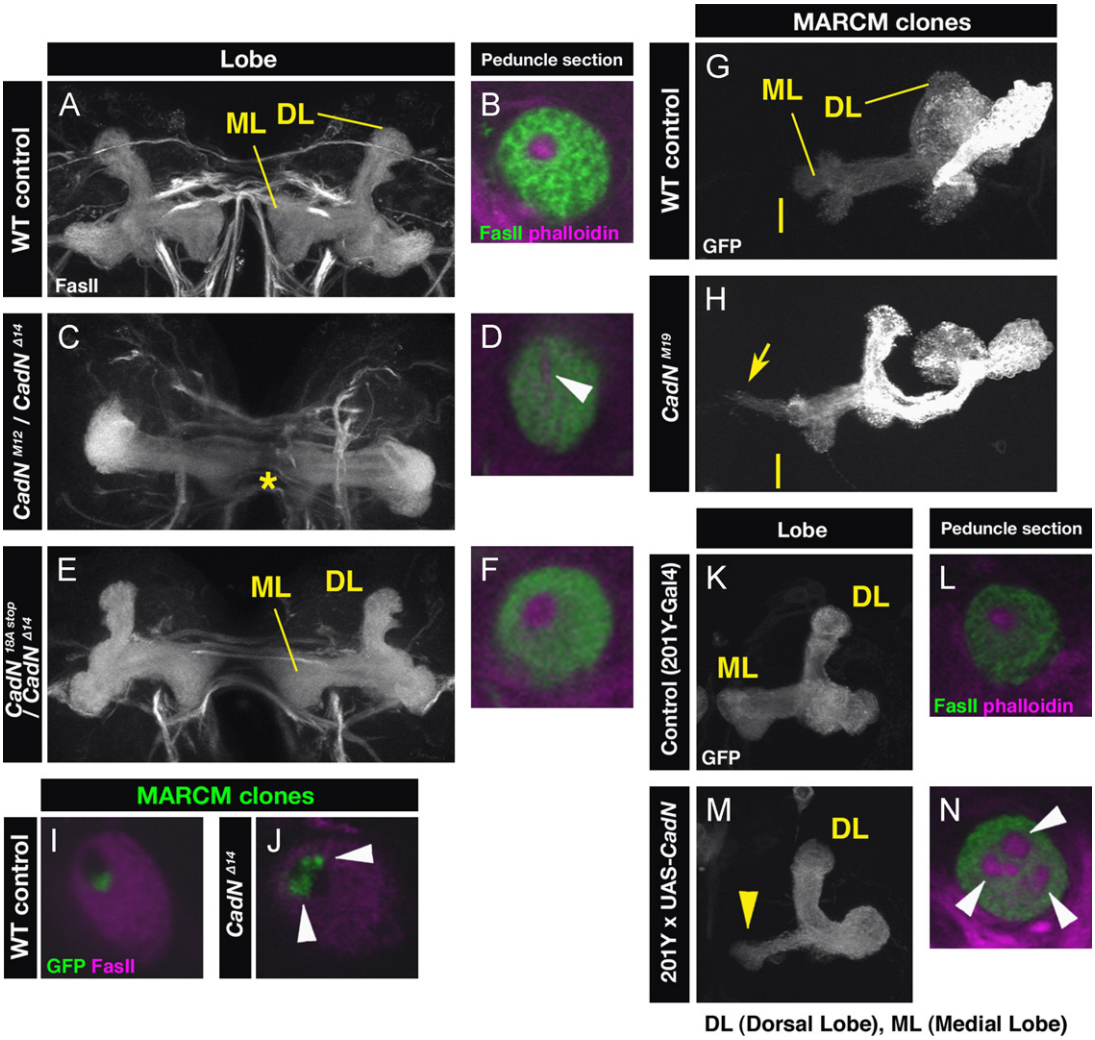

Fig. 3. CadN is required for axon guidance of MB neurons. (A, C, and E) Z-stacks showing the third instar larval MB lobes stained with anti-Fas II (white). (A) Wild type. (C) $CadN^{M12}/CadN^{\Delta 14}$. Medial lobes are fused across the midline (star) and dorsal lobes are missing. (E) $CadN^{18A\ stop}/CadN^{\Delta 14}$ showing normal MB morphology. (B, D, and F) Peduncle sections stained with anti-FasII (green) and phalloidin (magenta). (B) Wild type. (D) $CadN^{M12}/CadN^{\Delta 14}$. Arrowhead indicates the small core visualized with phalloidin. (F) $CadN^{18A\ stop}/CadN^{\Delta 14}$ exhibiting a normal core. (G and H) MARCM analysis showing wild-type Nb clones (G) and $CadN^{M19}$ Nb clones (H). The brain midline is indicated by a vertical bar. Arrow indicates the overextension of the medial lobe beyond the midline. (I and J) MARCM analysis. Peduncle sections. Clones (green) of developing neurons and anti-FasII (magenta). (I) Wild-type Nb clones have a unified bundle within the core. (J) $CadN^{\Delta 14}$ Nb clones. Mutant axons are defasciculated within the core (arrowheads). (K–N) Overexpression analysis using 201Y Gal4. Z-stacks of lobes with mCD8GFP (white) (K and M), and single sections of peduncles stained with anti-FasII (green) and phalloidin (magenta) (L and N). (K and L) 201Y control. (M and N) CadN overexpression using 201Y. The medial lobe becomes very thin (arrowhead in M) and the core axons are split into several distinct bundles (arrowheads in N) in the CadN overexpression.

molecules such as DLG and SYN in the larval calyx (Control, 0/24; GOF, 24/24) (Suppl. Fig. 4). Thus, downregulation of CadN expression level is likely to be required for proper formation of dendritic endings.

CadN expression shifts from axons to synapses during development of the neuromuscular system

To test whether the developmental changes in CadN expression and function are specific for MB neurons or are commonly found in other neural circuits of *Drosophila*, we examined the embryonic/larval neuromuscular system. Axons of motoneurons exiting the ventral nerve cord enter two distinct nerve roots, the intersegmental nerve (ISN) and segmental nerve. Motor axons remain within these nerves until they reach their target muscle fields, where they turn away from the nerve bundle and form synapses on the appropriate muscle fibers. Intense CadN immunoreactivity was detected throughout the developing axons of motoneurons (arrows in Fig. 5A) and within growth cones projecting onto muscles (arrowheads in Fig. 5A). We also detected CadN immunoreactivity in fibrous structures, likely muscle myopodia, adjacent to growth cones (Fig. 5A′).

In contrast to axonal CadN localization in embryonic motoneurons, functionally mature motoneurons of third instar larvae exhibited reduced levels of CadN expression in their axonal shafts (arrows in Fig. 5B), while punctate accumulation was clearly observed at Type I NMJs (brackets in Fig. 5B). Double staining with anti-CadN and the active zone marker, anti-Bruchpilot (BRP), revealed CadN expression adjacent to and partially overlapping presynaptic active zones (Fig. 5C). Similarly, high-magnification images of boutons stained with anti-GluRIIA demonstrated CadN accumulations surrounding GluR clusters on postsynaptic muscle (arrowheads in Fig. 5D and E). Furthermore, these postsynaptic CadN accumulations were adjacent to microzones on the presynaptic membrane stained with anti-HRP (arrows in Fig. 5D and E), supporting the notion that N-cadherin is important for the homophilic interaction between presynaptic and postsynaptic sites (Suzuki and Takeichi, 2008). Thus, similarly to MB neurons, motoneurons showed temporal changes in CadN expression and

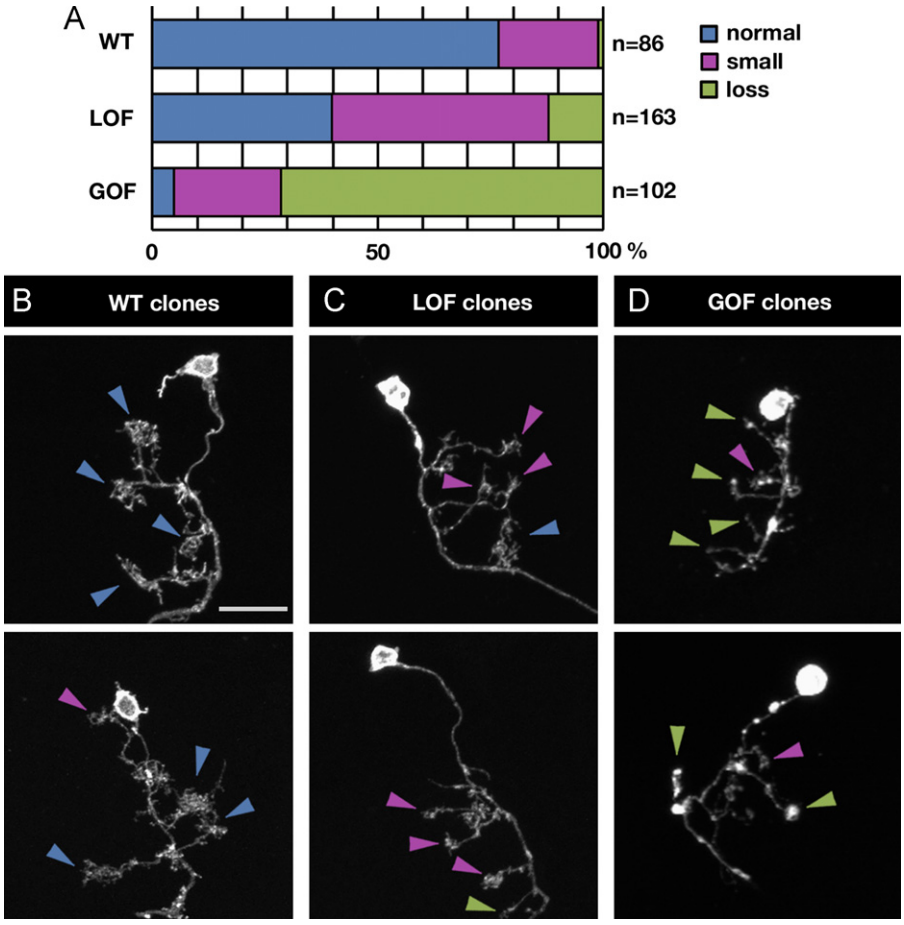

Fig. 4. CadN regulates the fine processes of MB dendritic endings. (A–D) MARCM analysis with single or two-cell clones. (A) Quantification of the morphology of dendritic endings in clones. "Normal" represents the large dendritic ending protruding a 4-μm-diameter circle. "Small" represents the small dendritic ending with shortened fine processes, fitting the same circle. "Loss" represents dendritic endings completely losing fine processes. LOF, loss-of-function by $CadN^{M19}$. GOF, gain-of-function by CadN overexpression. The total number of dendritic endings examined is indicated in the graph. Differences between controls and LOF/GOF are significant ($p < 0.001$, Chi-squared test). (B–D) Clones (white). Blue arrowheads, "normal" dendritic endings; magenta arrowheads, "small" dendritic endings; and green arrowheads, "loss" dendritic endings. (B) Wild-type single-cell clones. (C) $CadN^{M19}$ single-cell clones. (D) Single-cell clones with CadN overexpression. Scale bar: 10 μm in (B), applies also to (C and D).

subcellular distribution; CadN, initially distributed along entire axons of embryonic motoneurons, was later downregulated and concentrated at perisynaptic regions in mature motoneurons.

CadN functions in motor axon guidance, NMJ growth, and GluR clustering

Given the similar developmental pattern of expression to MB neurons, CadN may also be necessary for correct motor axon patterning. We focused on the ISNb pathway that leaves the ISN and forms characteristic projections onto the ventrolateral muscle field (Fig. 6A). Motor axon phenotypes were analyzed in embryos from stage 16 to early stage 17 by scoring the projection of axon stained with anti-FasII antibody in A2–A7 segments. In wild type, almost all ISNb projections (94% of hemisegments, 34/36) crossed the internal face of muscle 13 to reach the ventral edge of muscle 12 (arrow in Fig. 6A). In the *CadN* null mutant $CadN^{M19}/CadN^{\Delta 14}$, 31% (18/58) of ISNb hemisegments displayed strong axon guidance phenotypes; four axons (22%) failed to innervate muscle 12 and instead projected to another muscle (Fig. 6B), four axons (22%) entered muscle 12 but targeted a transverse nerve (Fig. 6C), six axons (33%) failed to leave the ISN pathway and innervated muscle 12 from the dorsal side (Fig. 6D), and four axons (22%) exhibited a stall phenotype in which the ISNb was truncated ventral to muscle 13 (data not shown). These diverse phenotypes suggest that CadN is required at multiple steps in motor axon pathfinding.

Accumulation of CadN at the presynaptic and the adjacent postsynaptic sites suggests that CadN is involved in synaptogenesis. To examine this, we used hypomorphic $CadN^{M12}$ and $CadN^{18A\ stop}$ alleles in transheterozygous combinations with $CadN^{\Delta 14}$. Note that axonal projection patterns of motoneurons in these hypomorphic mutants were normal at the third instar larval stage (Suppl. Fig. 5). Although $CadN^{M12}$ mutant boutons showed normal morphology (Fig. 6G), $CadN^{18A\ stop}$ mutant boutons were smaller and irregularly shaped compared with wild-type boutons (Fig. 6E and F, and Suppl. Fig. 6A and B), suggesting that the *CadN* isoforms containing exon 18a are essential for regulating bouton growth. We also investigated whether *CadN* mutations affect synaptic organization by staining NMJs with anti-GluRIIA and quantifying the mean surface area of postsynaptic GluR clusters. The expression level of GluRs was reduced in $CadN^{18A\ stop}$ mutants compared with wild types (Suppl. Fig. 6A and B). The intensities of GluR staining were rendered in 3D surface visualization (Fig. 6E1–G1). The surface rendering revealed that the $CadN^{18A\ stop}$ mutation resulted in a significant reduction in receptor field surface area compared to wild types, while $CadN^{M12}$ mutants were normal (Wild type: $4.10 \pm 0.194\ \mu m^2$ SD, $n=8$; $CadN^{18A\ stop}$: 3.25 ± 0.357, $n=10$; $CadN^{M12}$: 4.22 ± 0.283, $n=10$) (Fig. 6H). We also examined active zone formation with anti-BRP staining; however, no obvious alteration was observed in $CadN^{18A\ stop}$

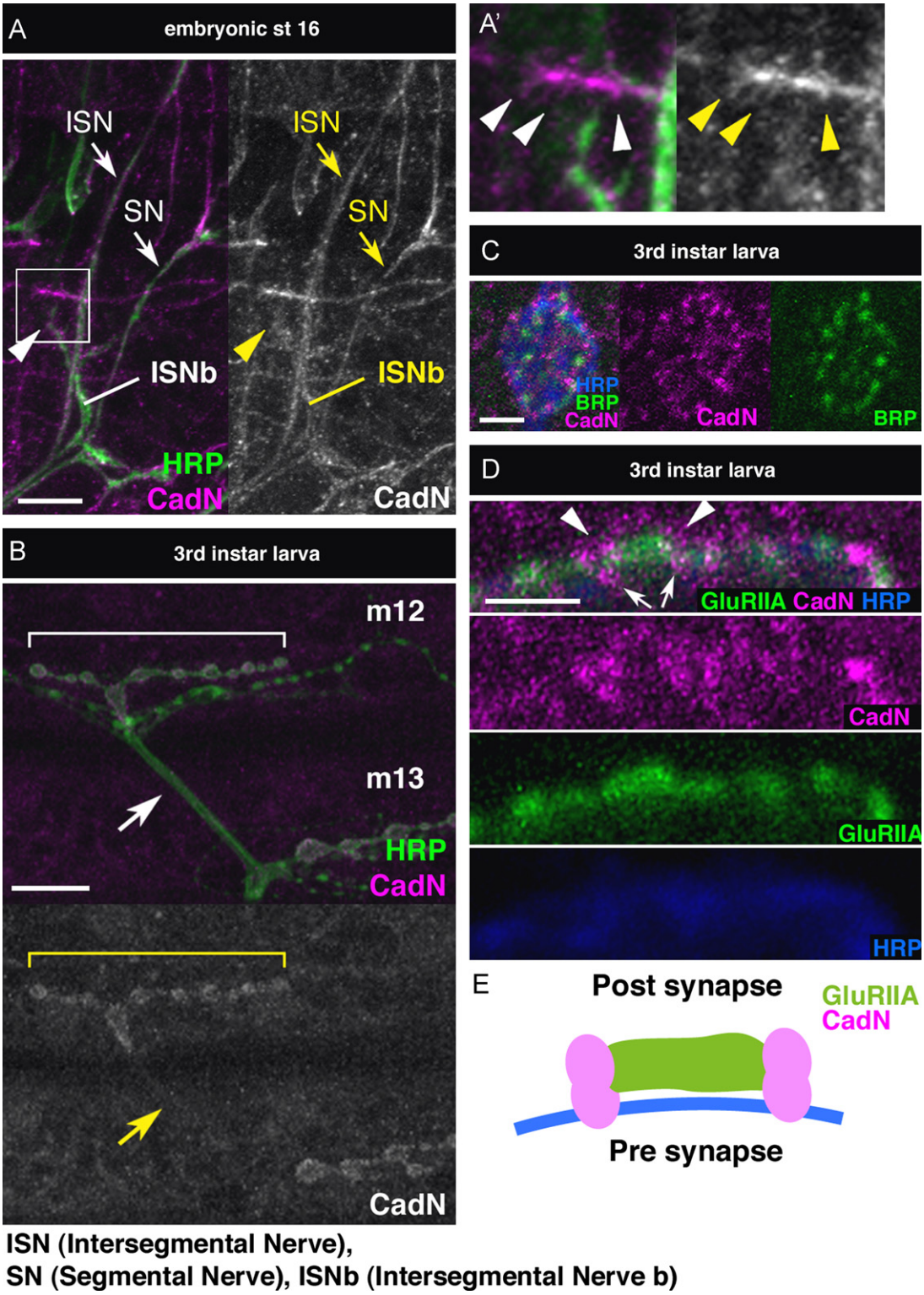

Fig. 5. CadN expression patterns in motoneurons and neuromuscular junctions (NMJs). (A) Stage 16 embryo stained with anti-HRP (green) and anti-CadN (magenta). Arrowheads, the growth cones; arrows, the motor axons. (A′) A high-magnification image of the inset in (A). Arrowheads indicate fibrous structures extended from muscle 12. (B) NMJs at muscles 12/13 at the third instar stage stained with anti-HRP (green) and anti-CadN (magenta). CadN is accumulated on the Type Ib boutons (brackets) but absent on axons (arrows). (C) A high-magnification image of Type Ib boutons stained with anti-HRP (blue), anti-BRP (green), and anti-CadN (magenta). CadN staining overlaps with BRP signals. (D) A high-magnification image of Type Ib bouton stained with anti-HRP (blue), anti-GluRIIA (green), and anti-CadN (magenta). Arrowheads indicate the localization of postsynaptic CadN on the edge of GluR field. Zones of postsynaptic CadN (arrowheads) are present in opposition to zones of presynaptic CadN (arrows). (E) A diagram summarizing localization patterns of CadN (magenta) and GluRIIA (green). Scale bars: 10 μm in (A); 20 μm in (B); 2 μm in (C and D).

mutants (Suppl. Fig. 6C and D), indicating that 18a-containing CadN isoforms are required for the proper accumulation of GluR receptors but not for presynaptic active zone formation.

Consistent with the synaptic phenotypes, CadN immunoreactivity at the NMJ was considerably reduced in the *CadN*$^{18A\ stop}$ mutants (Fig. 6I and J). Moreover, a similar expression profile was

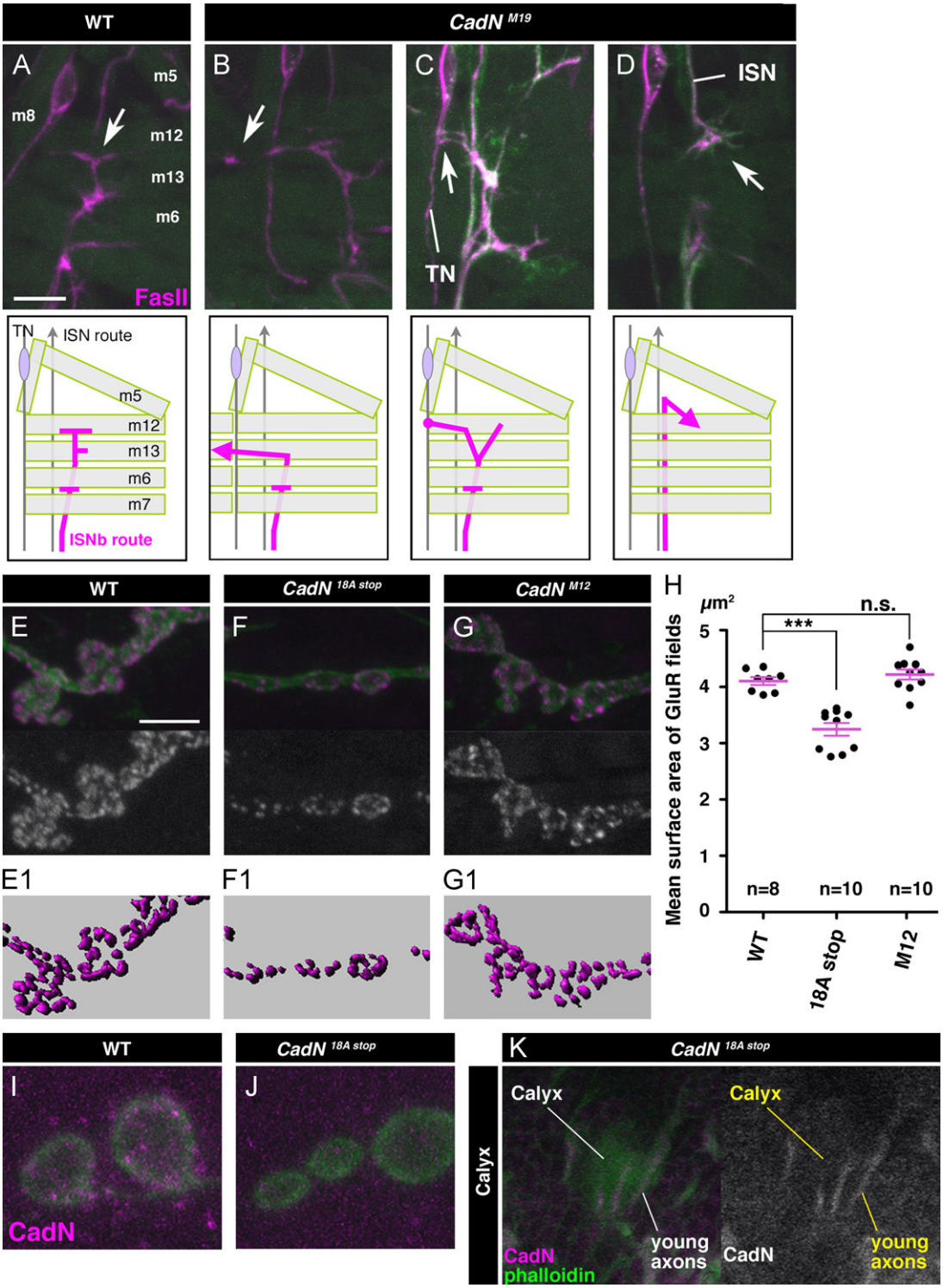

Fig. 6. CadN is required for axon guidance and synaptic growth of motoneurons. (A–D) ISNb pathways (arrowheads) at late stage 16/early stage 17 embryos. Anti-HRP (green) and anti-FasII (magenta). Diagrams show the observed projection patterns of ISNb axons. (A) Wild type. Positions of different muscles are indicated (m5, m6, m12, and m13). (B–D) $CadN^{M19}/CadN^{\Delta 14}$. Examples of the mistargeting (B and C) and the misrouting (D) phenotypes. (E–G) Type Ib boutons at muscle 4 of A3 segment at the third instar stage. Anti-HRP (green) and anti-GluRIIA (magenta). (E1–G1) 3D rendering images of GluR fields shown in (E–G). (E and E1) Wild type. (F and F1) $CadN^{18A\ stop}/CadN^{\Delta 14}$, with the reduced bouton size and GluR field. (G and G1) $CadN^{M12}/CadN^{\Delta 14}$, with the normal morphology of NMJs. (H) The mean surface area (μm^2) of GluR fields. Each of the plotted mean values is calculated based on at least 50 receptor fields captured in separate images. The total number of individual samples is indicated in the graph. Error bar, SD. n.s., Not significant; $^{***}p < 0.001$ (ANOVA with Dunnett's multiple comparison test). (I and J) NMJs at muscle 4 of A3 segment at the third instar stage. Anti-HRP (green) and anti-CadN (magenta). (I) Wild type. (J) $CadN^{18A\ stop}/CadN^{\Delta 14}$. (K) CadN immunoreactivity (magenta) in the MB calyx region of $CadN^{18A\ stop}/CadN^{\Delta 14}$ larva at the third instar stage. Developing MB axons are visualized with phalloidin (green). (A–G) Z-stacks. (I–K) single sections. Scale bars: 10 μm in (A), applies also to (B–D); 5 μm in (E), applies also to (F and G). Abbreviations: ISN, intersegmental nerve; ISNb, intersegmental nerve b; TN, transverse nerve.

observed in the larval MB; CadN signals in *CadN*$^{18A\ stop}$ mutants were reduced in the mature MB calyx but prominent in developing axons (Fig. 6K and compare with Fig. 1D). Since the anti-CadN antibody recognizes an epitope present in all isoforms, the selective loss of CadN signals in *CadN*$^{18A\ stop}$ mutants indicates that 18a-containing isoforms are dominant in mature motoneurons and MB neurons.

A cell-autonomous developmental switch in CadN expression

To investigate the mechanisms of switching in CadN expression, we tested whether extrinsic cues from synaptic contacts are required for CadN expression changes using a low-density primary cell culture system. In this system, neurons extend axons and develop presynaptic specializations without making synaptic contact with other cells, concomitantly with normal control of expression of cell surface proteins such as Robo3 and Derailed (Drl) (Katsuki et al., 2009). Cells were dissociated from mid-stage embryos and cultures were fixed every 6 h after seeding, followed by staining with anti-CadN and anti-SYN (Fig. 7). Neurons were identified by expression of *elav*-Gal4 > mCD8GFP, and SYN expression was measured to determine the differentiation state of presynaptic specializations. After 6 h in culture, neurons expressed high levels of CadN along axons (Fig. 7A and C) but lacked detectable SYN expression (Fig. 7B–D), indicating their immature state. After 18 h in culture, CadN expression started to diminish and showed a punctate pattern (Fig. 7A and E), while SYN expression was upregulated and appeared as puncta in distal axons (Fig. 7B and E), consistent with neuronal maturation. High-magnification images revealed CadN puncta colocalized with SYN puncta in distal axons (Fig. 7F) in addition to solitary CadN puncta in proximal axons, suggesting that CadN is present in presynaptic specialization. As culture duration increased to 36 h, diffuse CadN immunoreactivity continued to decrease (Fig. 7A and G), while punctate SYN and CadN colocalization in distal axons increased further (Fig. 7B and H). Thus, CadN downregulation and changes in subcellular localization can take place in the absence of synaptic inputs from other cells.

Downregulation of CadN expression can be triggered by cation influx

Spontaneous intracellular ion transients can occur independently of synaptic input in developing neurons and the resulting changes in intracellular ionic concentrations act as triggers for neuronal development (Moody, 1998; Spitzer, 2002, 2006). To test if cation influx in developing *Drosophila* neurons affects CadN expression, we examined flies expressing the *Drosophila* heat-activated cation

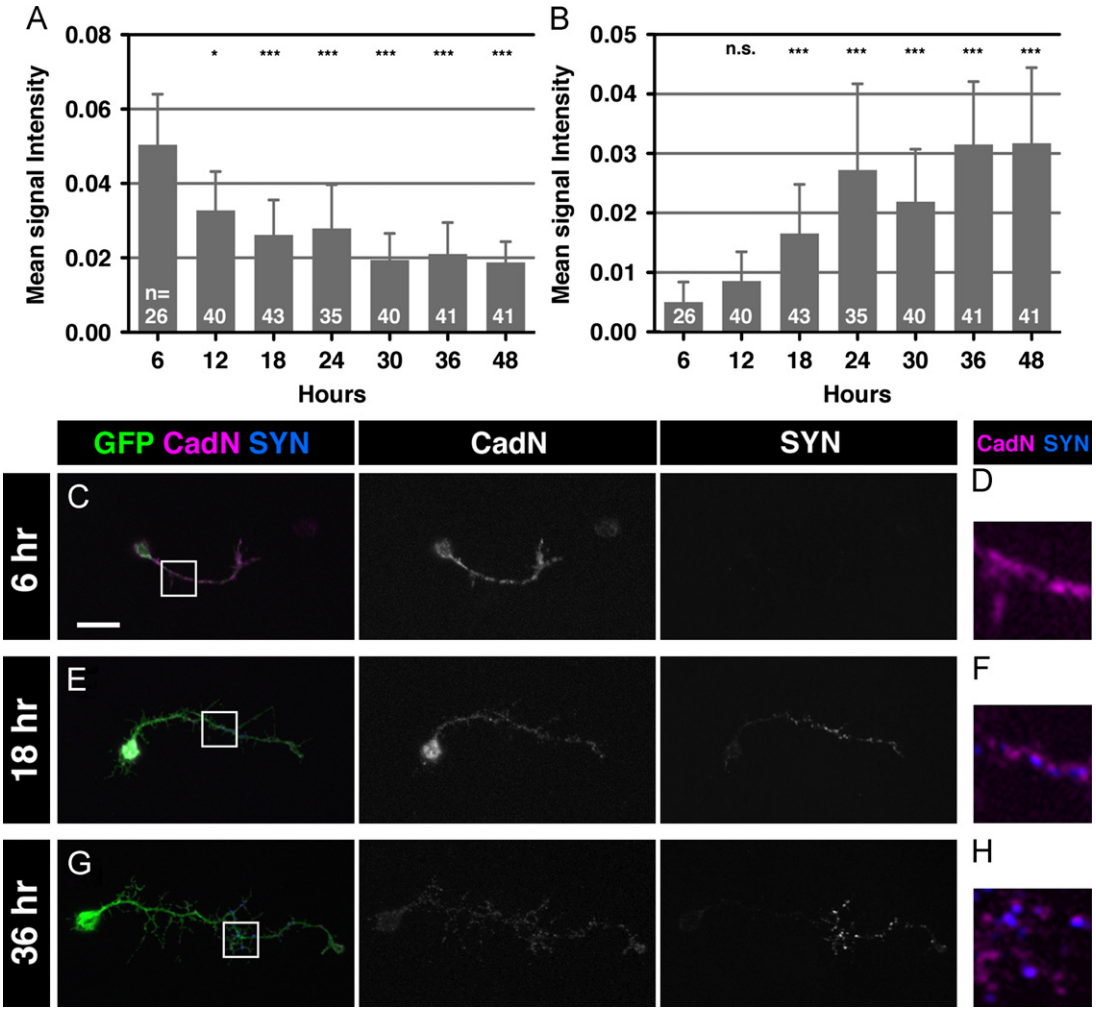

Fig. 7. Intrinsic control of CadN expression in *Drosophila* cultured neurons. (A and B) The mean signal intensity of anti-CadN (A) and anti-SYN (B) immunostaining in cultured neurons. The total number of neurons examined is indicated in the bar. n.s., Not significant; $^{*}p < 0.05$; $^{***}p < 0.001$ (Kruskal–Wallis test with Dunn's multiple comparison against 6 h). Error bar, SD. (C–H) Single sections of cultured neurons stained with anti-CadN (magenta) and anti-SYN (blue). Neurons were visualized with *elav*-Gal4 > UAS-*CD8GFP* (green). (C and D) 6 h culture. (E and F) 18 h culture. (G and H) 36 h culture. (D, F, and H) High-magnification images corresponding to the insets in (C, E, and G), respectively. Scale bar: 10 μm in (C), applies also to (E and G).

channel dTRPA1, which allows nonselective cation influx and causes neuronal depolarization (Hamada et al., 2008; Pulver et al., 2009). To activate dTRPA1 in MB neurons, third instar larvae carrying UAS-*dTRPA1* and OK107-Gal4 were grown at nonpermissive temperature for 3, 6, or 9 h. In MBs dissected from larvae grown at permissive temperature and from minimal control larvae with heat shock alone in the absence of TRPA1, CadN displayed wild-type expression patterns; strong expression in cell bodies and core axons of developing neurons and low expression in mature neurons (Fig. 8A–D). Activation of dTRPA1 for 3 h did not induce any observable changes in CadN expression in MB neurons (data not shown), while heat-activation for 6 or 9 h caused a reduction in CadN expression level in developing neurons similar to that observed in wild-type mature neurons (6 h, data not shown; 9 h, Fig. 8E and F). The result could not be explained by loss of developing neurons because the expression of Neurotactin (NRT), another CAM (Hortsch et al., 1990; de la Escalera et al., 1990), was strongly expressed in most inner core axons as in wild type, indicating an intact production of neurons (Fig. 8A–F). Moreover, the reduced expression of CadN induced by dTRPA1 activation did not affect formation of MB substructures such as the fasciculation of developing neurons and the branching pattern (Fig. 8F and data not shown). Thus, sustained

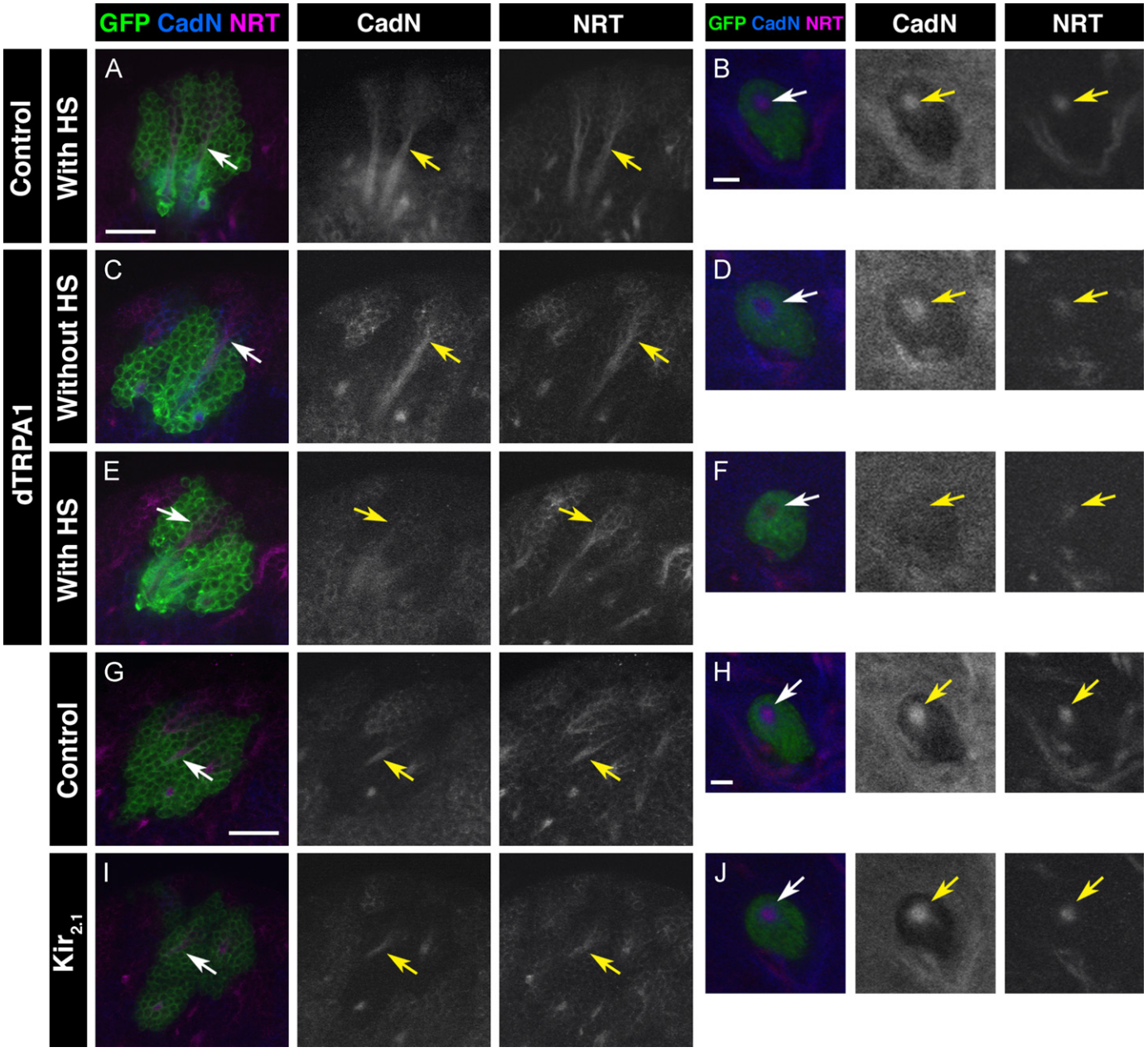

Fig. 8. Activation of the dTRPA1 cation channel can downregulate CadN expression in developing MB neurons. (A–J) Single sections through MBs stained with anti-CadN (blue) and anti-NRT (magenta). MB cell bodies (A, C, E, G, and I) and peduncles (B, D, F, H, and J). Arrows, developing neurons. (A and B) Minimal control MB after 9 h heat shock in the absence of dTRPA1. UAS-*mCD8GFP* (green) was driven by OK107. Note that strong NRT expression is usually detected in the youngest neurons located in the most inner core of the peduncle. (C–F) UAS-*mCD8GFP* (green) and UAS-*dTRPA* were driven by OK107. (C and D) MB without heat shock. CadN and NRT expressions were not affected. (E and F) MB after 9 h activation of dTRPA1 by heat shock. The activation of dTRPA1 downregulates CadN expression but not NRT expression in developing neurons. (G and H) Control MB. UAS-*mCD8GFP* (green) was driven by OK107. (I and J) $Kir_{2.1}$ overexpression. UAS-*mCD8GFP* (green) and UAS-$Kir_{2.1}$ were driven by OK107. CadN and NRT expressions were not affected in both developing and mature neurons. Scale bars: 20 μm in (A), applies also to (C and E); 5 μm in (B), applies also to (D and F); 20 μm in (G), applies also to (I); 5 μm in (H), applies also to (J).

dTRPA1 activation can induce precocious downregulation of CadN in developing MB neurons (see summary indicated in Suppl. Fig. 7). It also indicates that not all CAMs are affected equally by dTRPA1 activation (Suppl. Fig. 7).

Because dTRPA1 can induce cation influx and resulting depolarization, we examined whether neuronal depolarization is required for downregulation of CadN expression in MB neurons. To repress neuronal excitability, we overexpressed a human inwardly rectifying K^+ channel ($Kir_{2.1}$), which is known to induce hyperpolarization and eliminate action potentials in *Drosophila* (Baines et al., 2001). $Kir_{2.1}$ overexpression in MB neurons did not affect CadN expression patterns (Fig. 8G–J). The same result was confirmed by an alternative neuronal suppression technique using *Drosophila* open rectifier K^+ channel (dORK), whose overexpression silences action potentials in *Drosophila* (Nitabach et al., 2002) (data not shown). These results indicate that neuronal depolarization is dispensable for the developmental switch in CadN expression levels. Taken together, these results suggest that developmental switching of CadN expression levels might be controlled by intracellular ionic concentrations.

Discussion

N-cadherins participate in multiple aspects of neural circuit formation, but it remains unclear how these phase-specific functions are coordinated. In this paper, we show that *Drosophila* CadN exhibits distinct expression patterns in developing versus mature neurons of the MB and neuromuscular system, with ubiquitous expression in developing axons and highly restricted synaptic localization in differentiated neurons (Figs. 1, 2, and 5). Mutant analyses reveal that CadN is required for proper axonal pathfinding and fasciculation in developing neurons (Figs. 3 and 6) and for formation of normal synapses by more mature neurons (Figs. 4 and 6). We examined CadN expression in dilute neuronal cultures and found that downregulation and relocalization can be mediated by cell-intrinsic programs and do not require synaptic contacts with other cells (Fig. 7). These intrinsic programs may involve a developmentally regulated influx of cations, since ectopic expression of a nonselective cation channel prematurely induces transition in the CadN expression pattern *in vivo* (Fig. 8). Our findings provide a plausible mechanism for the execution of multiple developmental functions by CadN in the same neuronal population.

CadN has multiple stage-specific functions in individual neurons

Our systematic mutant analysis revealed diverse functions of CadN in MB neurons and motoneurons. In MB development, CadN participates in the fasciculation and proper extension of developing axons as well as affecting the elaboration of fine dendritic processes in the calyx (Figs. 3 and 4). In neuromuscular networks, CadN is required at multiple steps in embryonic motor axon pathfinding and also for bouton growth and GluR clustering in larval NMJs (Fig. 6). A fundamental question is how CadN exhibits such diverse functions. One possibility is that the dynamic changes of CadN expression in the course of neuronal development allow CadN to act at different cellular and developmental contexts. For example, high levels of expression throughout the axons in developing neurons might be required for fasciculation and extension of axons, while highly restricted expression at synaptic sites in mature neurons might be involved in establishment and maintenance of synapses. Indeed, manipulation of CadN expression levels and timing affect both axon guidance and synapse formation in MBs (Fig. 3K–N and Suppl. Fig. 4). Thus, although our study does not provide direct evidence to show that distinct localization is responsible for different functions of CadN, these phenotypic analyses, together with expression analyses, underscore the importance of CadN expression controls.

Spatial and temporal regulation of CadN expression within a neuron may not be the only mechanism for the multi-functionality of CadN. Other cell surface proteins might work cooperatively with CadN to confer distinct functional properties on the CadN adhesion system. In the peduncle regions of the MB, loss of CadN resulted in defasciculation of core axons with low penetrance (Fig. 3), suggesting that adhesion among core axons is regulated by the axonal localization of CadN. Similar MB defasciculation and low-penetrance defects are observed in *Dscam* (encoding the Down Syndrome CAM) and *Ptp69D* (encoding a receptor tyrosine phosphatase (RPTP)) mutants. Similarly to CadN, these proteins are selectively expressed on core axons (Zhan et al., 2004; Kurusu and Zinn, 2008). Other MB defects caused by *CadN* mutations included overextension phenotypes, in which medial lobe axons leave their bundles and extend across the midline into the contralateral medial lobe (Fig. 3). This suggests that CadN negatively regulates axon extension, perhaps by maintaining strong interaxonal adhesion. Similar phenotypes are found in *drl* (Moreau-Fauvarque et al., 1998) and *Lar* mutants (Kurusu and Zinn, 2008). Drl is a receptor tyrosine kinase, and LAR is an RPTP. CadN and LAR are also required for targeting of *Drosophila* R1-6 retinal axons (Clandinin et al., 2001; Prakash et al., 2009). Thus, it is possible that CadN cooperatively functions with these proteins to exert multiple roles during circuit formation.

CadN was also required for several aspects of synaptogenesis, including synaptic terminal growth and postsynaptic receptor clustering (Figs. 4 and 6). The *CadN* mutations perturbed the elaboration of fine processes on MB dendrites and the morphology of NMJs, deficits reminiscent of the perturbed spine morphogenesis in hippocampal neurons expressing dominant negative N-cadherin (Togashi et al., 2002; Bozdagi et al., 2004; Okamura et al., 2004). These data suggest that CadN/N-cadherin may have a conserved role in the growth of synaptic terminals. We also demonstrated the selective expression of CadN 18a isoforms in mature neurons (Fig. 6). Yonekura et al. (2006) showed that 18a isoforms had lower adhesive activity than 18b isoforms and hypothesized that the weak cell–cell interaction mediated by 18a isoforms allows for synaptic changes in morphology (plasticity), while the strong interaction by 18b isoforms contributes to axonal guidance mechanisms that produce stable neuronal circuits. Our data support this notion, but the exact functions of 18a and 18b isoforms remain to be elucidated.

Our data suggest an important role for CadN in clustering of postsynaptic GluRs, again consistent with N-cadherin function in vertebrates. Vertebrate N-cadherin is known to be concentrated at the edges of synaptic areas (Yamagata et al., 1995; Fannon and Colman, 1996; Uchida et al., 1996; Benson and Tanaka, 1998; Elste and Benson, 2006). N-cadherin interacts with AMPA receptors, forming complexes that can stimulate synaptic development (Nuriya and Huganir, 2006; Saglietti et al., 2007). Other GluRs, such as NMDA and kainate receptors, may also form complexes with N-cadherins (Husi et al., 2000; Coussen et al., 2002). These data suggest that regulation of receptor clustering is a conserved function of CadN/N-cadherin, at least at glutamatergic synapses. Furthermore, we showed that *CadN* mutations affect the elaboration of MB dendritic endings that receive cholinergic inputs from olfactory PNs (Fig. 4; Yasuyama et al., 2002). Thus, it would be interesting to know whether CadN/N-cadherin is involved in the organization of other types of receptors such as the acetylcholine receptor.

Potential regulatory mechanisms directing developmental switches in CadN expression and subcellular localization

Our data show that CadN expression patterns change during development. The differential sub-cellular distributions of CAMs

are sometimes directed by their amino acid sequences. Proteolytic cleavage of the N-terminal prodomain is involved in N-cadherin targeting vertebrate synapses, but the *Drosophila CadN* gene does not encode the prodomain (Koch et al., 2004; Latefi et al., 2009). DSCAM splice isoforms carrying different transmembrane domains are targeted to distinct subcellular domains of neurons (Wang et al., 2004). CadN isoforms contain one of the two different transmembrane domains encoded by exon 18a or 18b, and our mutant analysis revealed that the $CadN^{18A\ stop}$ mutation reduced CadN immunoreactivity in mature synapses of the MB and at NMJs, but not in developing neurons (Fig. 6). This suggests that 18a-containing isoforms are predominantly expressed in synaptic regions. Similarly, enrichment of 18a isoforms was detected in adult eyes, while the 18b isoforms dominated in developing eye discs (Nern et al., 2005; Yonekura et al., 2006). Thus, the developmental transition from the 18b to the 18a isoforms is probably common in the *Drosophila* nervous system. Although 18a- and 18b-containing isoforms fused to GFP reporters show no difference in axon versus dendrite localization in both MB neurons and motoneurons (Hsu et al., 2009), the difference between CadN transmembrane domains might define microdomains to be localized in subcellular regions. Alternatively, a trans-acting mechanism that differs between developing and mature neurons alters CadN subcellular localization.

What are the mechanisms that trigger the developmental switch in CadN expression? Our low-density culture experiment demonstrated that synaptic inputs are not required for downregulation of CadN expression (Fig. 7). Neuronal depolarization was also dispensable for the downregulation, but activation of the temperature-sensitive cation channel, dTRPA1, was sufficient to downregulate CadN expression in developing MB neurons *in vivo* (Fig. 8). This suggests that a developmentally regulated cation influx pathway triggers the developmental transition in CadN expression. Calcium influx is the signal most likely to be responsible, because it is a critical signal that triggers many neurodevelopmental events (Spitzer, 2002, 2006). We therefore hypothesize that spontaneous calcium transients in developing neurons are responsible for downregulation of CadN expression. Some embryonic motoneurons do show small inward calcium currents during specific developmental stages (Baines and Bate, 1998; Rohrbough et al., 2003) and cultured neurons derived from the developing MB can generate spontaneous calcium transients (Jiang et al., 2005). In vertebrates, spontaneous calcium transients occur prior to synapse formation (Moody, 1998; Spitzer, 2002, 2006). Furthermore, patterned electrical stimulation, presumably causing voltage-dependent calcium influx, can downregulate N-cadherin expression in cultured dorsal root ganglion neurons (Itoh et al., 1997). Future microfluorometric imaging experiments and cell signaling assays are required to examine the cation or calcium dependence of CadN regulation and targeting.

Acknowledgments

We thank Drs. S.L. Zipursky, T.R. Clandinin, L. Luo, R. Okada, and T. Uemura as well as the Bloomington Stock Center and Developmental Studies Hybridoma Bank for generously providing the fly stocks, antibodies, and staining protocol. We also thank members of the Suzuki and Zinn groups for helpful discussions, A. Oishi and M. Taniguchi for technical assistance, and Y. Hiromi for the use of his laboratory to perform cell culture experiments. This work was supported by Grants-in-Aid for Scientific Research from MEXT Japan, Naito Foundation, and The Nakajima Foundation to M.K., and by NIH Grant RO1 NS062821 to K.Z.

Appendix A. Supporting information

Supplementary data associated with this article can be found in the online version at http://dx.doi.org/10.1016/j.ydbio.2012.04.006.

References

Baines, R.A., Bate, M., 1998. Electrophysiological development of central neurons in the *Drosophila* embryo. J. Neurosci. 18, 4673–4683.
Baines, R.A., Uhler, J.P., Thompson, A., Sweeney, S.T., Bate, M., 2001. Altered electrical properties in *Drosophila* neurons developing without synaptic transmission. J. Neurosci. 21, 1523–1531.
Benson, D.L., Tanaka, H., 1998. N-cadherin redistribution during synaptogenesis in hippocampal neurons. J. Neurosci. 18, 6892–6904.
Bozdagi, O., Shan, W., Tanaka, H., Benson, D.L., Huntley, G.W., 2000. Increasing numbers of synaptic puncta during late-phase LTP: N-cadherin is synthesized, recruited to synaptic sites, and required for potentiation. Neuron 28, 245–259.
Bozdagi, O., Valcin, M., Poskanzer, K., Tanaka, H., Benson, D.L., 2004. Temporally distinct demands for classic cadherins in synapse formation and maturation. Mol. Cell. Neurosci. 27, 509–521.
Broadbent, I.D., Pettitt, J., 2002. The *C. elegans* hmr-1 gene can encode a neuronal classic cadherin involved in the regulation of axon fasciculation. Curr. Biol. 12, 59–63.
Clandinin, T.R., Lee, C.H., Herman, T., Lee, R.C., Yang, A.Y., Ovasapyan, S., Zipursky, S.L., 2001. *Drosophila* LAR regulates R1–R6 and R7 target specificity in the visual system. Neuron 32, 237–248.
Coussen, F., Normand, E., Marchal, C., Costet, P., Choquet, D., Lambert, M., Mege, R.M., Mulle, C., 2002. Recruitment of the kainate receptor subunit glutamate receptor 6 by cadherin/catenin complexes. J. Neurosci. 22, 6426–6436.
de la Escalera, S., Bockamp, E.O., Moya, F., Piovant, M., Jimenez, F., 1990. Characterization and gene cloning of neurotactin, a *Drosophila* transmembrane protein related to cholinesterases. EMBO J. 9, 3593–3601.
Doherty, P., Rowett, L.H., Moore, S.E., Mann, D.A., Walsh, F.S., 1991. Neurite outgrowth in response to transfected N-CAM and N-cadherin reveals fundamental differences in neuronal responsiveness to CAMs. Neuron 6, 247–258.
Doherty, P., Skaper, S.D., Moore, S.E., Leon, A., Walsh, F.S., 1992. A developmentally regulated switch in neuronal responsiveness to NCAM and N-cadherin in the rat hippocampus. Development 115, 885–892.
Elste, A.M., Benson, D.L., 2006. Structural basis for developmentally regulated changes in cadherin function at synapses. J. Comp. Neurol. 495, 324–335.
Fannon, A.M., Colman, D.R., 1996. A model for central synaptic junctional complex formation based on the differential adhesive specificities of the cadherins. Neuron 17, 423–434.
Hamada, F.N., Rosenzweig, M., Kang, K., Pulver, S.R., Ghezzi, A., Jegla, T.J., Garrity, P.A., 2008. An internal thermal sensor controlling temperature preference in *Drosophila*. Nature 454, 217–220.
Hortsch, M., Patel, N.H., Bieber, A.J., Traquina, Z.R., Goodman, C.S., 1990. *Drosophila* neurotactin, a surface glycoprotein with homology to serine esterases, is dynamically expressed during embryogenesis. Development 110, 1327–1340.
Hsu, S.N., Yonekura, S., Ting, C.Y., Robertson, H.M., Iwai, Y., Uemura, T., Lee, C.H., Chiba, A., 2009. Conserved alternative splicing and expression patterns of arthropod N-cadherin. PLoS Genet. 5, e1000441.
Hummel, T., Zipursky, S.L., 2004. Afferent induction of olfactory glomeruli requires N-cadherin. Neuron 42, 77–88.
Husi, H., Ward, M.A., Choudhary, J.S., Blackstock, W.P., Grant, S.G., 2000. Proteomic analysis of NMDA receptor–adhesion protein signaling complexes. Nat. Neurosci. 3, 661–669.
Inoue, A., Sanes, J.R., 1997. Lamina-specific connectivity in the brain: regulation by N-cadherin, neurotrophins, and glycoconjugates. Science 276, 1428–1431.
Ito, K., Hotta, Y., 1992. Proliferation pattern of postembryonic neuroblasts in the brain of *Drosophila melanogaster*. Dev. Biol. 149, 134–148.
Itoh, K., Ozaki, M., Stevens, B., Fields, R.D., 1997. Activity-dependent regulation of N-cadherin in DRG neurons: differential regulation of N-cadherin, NCAM, and L1 by distinct patterns of action potentials. J. Neurobiol. 33, 735–748.
Iwai, Y., Hirota, Y., Ozaki, K., Okano, H., Takeichi, M., Uemura, T., 2002. DN-cadherin is required for spatial arrangement of nerve terminals and ultrastructural organization of synapses. Mol. Cell. Neurosci. 19, 375–388.
Iwai, Y., Usui, T., Hirano, S., Steward, R., Takeichi, M., Uemura, T., 1997. Axon patterning requires DN-cadherin, a novel neuronal adhesion receptor, in the *Drosophila* embryonic CNS. Neuron 19, 77–89.
Jiang, S.A., Campusano, J.M., Su, H., O'Dowd, D.K., 2005. *Drosophila* mushroom body Kenyon cells generate spontaneous calcium transients mediated by PLTX-sensitive calcium channels. J. Neurophysiol. 94, 491–500.
Jüngling, K., Eulenburg, V., Moore, R., Kemler, R., Lessmann, V., Gottmann, K., 2006. N-cadherin transsynaptically regulates short-term plasticity at glutamatergic synapses in embryonic stem cell-derived neurons. J. Neurosci. 26, 6968–6978.
Katsuki, T., Ailani, D., Hiramoto, M., Hiromi, Y., 2009. Intra-axonal patterning: intrinsic compartmentalization of the axonal membrane in *Drosophila* neurons. Neuron 64, 188–199.
Koch, A.W., Farooq, A., Shan, W., Zeng, L., Colman, D.R., Zhou, M.M., 2004. Structure of the neural (N-) cadherin prodomain reveals a cadherin extracellular domain-like fold without adhesive characteristics. Structure 12, 793–805.

Kurusu, M., Awasaki, T., Masuda-Nakagawa, L.M., Kawauchi, H., Ito, K., Furukubo-Tokunaga, K., 2002. Embryonic and larval development of the *Drosophila* mushroom bodies: concentric layer subdivisions and the role of fasciclin II. Development 129, 409–419.

Kurusu, M., Nagao, T., Walldorf, U., Flister, S., Gehring, W.J., Furukubo-Tokunaga, K., 2000. Genetic control of development of the mushroom bodies, the associative learning centers in the *Drosophila* brain, by the eyeless, twin of eyeless, and Dachshund genes. Proc. Natl. Acad. Sci. USA 97, 2140–2144.

Kurusu, M., Zinn, K., 2008. Receptor tyrosine phosphatases regulate birth order-dependent axonal fasciculation and midline repulsion during development of the *Drosophila* mushroom body. Mol. Cell. Neurosci. 38, 53–65.

Latefi, N.S., Pedraza, L., Schohl, A., Li, Z., Ruthazer, E.S., 2009. N-cadherin prodomain cleavage regulates synapse formation *in vivo*. Dev. Neurobiol. 69, 518–529.

Lee, C.H., Herman, T., Clandinin, T.R., Lee, R., Zipursky, S.L., 2001. N-cadherin regulates target specificity in the *Drosophila* visual system. Neuron 30, 437–450.

Lee, T., Lee, A., Luo, L., 1999. Development of the *Drosophila* mushroom bodies: sequential generation of three distinct types of neurons from a neuroblast. Development 126, 4065–4076.

Leiss, F., Groh, C., Butcher, N.J., Meinertzhagen, I.A., Tavosanis, G., 2009. Synaptic organization in the adult *Drosophila* mushroom body calyx. J. Comp. Neurol. 517, 808–824.

Masai, I., Lele, Z., Yamaguchi, M., Komori, A., Nakata, A., Nishiwaki, Y., Wada, H., Tanaka, H., Nojima, Y., Hammerschmidt, M., Wilson, S.W., Okamoto, H., 2003. N-cadherin mediates retinal lamination, maintenance of forebrain compartments and patterning of retinal neurites. Development 130, 2479–2494.

Matsunaga, M., Hatta, K., Nagafuchi, A., Takeichi, M., 1988. Guidance of optic nerve fibres by N-cadherin adhesion molecules. Nature 334, 62–64.

Moody, W.J., 1998. Control of spontaneous activity during development. J. Neurobiol. 37, 97–109.

Moreau-Fauvarque, C., Taillebourg, E., Boissoneau, E., Mesnard, J., Dura, J.M., 1998. The receptor tyrosine kinase gene linotte is required for neuronal pathway selection in the *Drosophila* mushroom bodies. Mech. Dev. 78, 47–61.

Nern, A., Nguyen, L.V., Herman, T., Prakash, S., Clandinin, T.R., Zipursky, S.L., 2005. An isoform-specific allele of *Drosophila* N-cadherin disrupts a late step of R7 targeting. Proc. Natl. Acad. Sci. USA 102, 12944–12949.

Nitabach, M.N., Blau, J., Holmes, T.C., 2002. Electrical silencing of *Drosophila* pacemaker neurons stops the free-running circadian clock. Cell 109, 485–495.

Nuriya, M., Huganir, R.L., 2006. Regulation of AMPA receptor trafficking by N-cadherin. J. Neurochem. 97, 652–661.

Okamura, K., Tanaka, H., Yagita, Y., Saeki, Y., Taguchi, A., Hiraoka, Y., Zeng, L.H., Colman, D.R., Miki, N., 2004. Cadherin activity is required for activity-induced spine remodeling. J. Cell Biol. 167, 961–972.

Pascual, A., Preat, T., 2001. Localization of long-term memory within the *Drosophila* mushroom body. Science 294, 1115–1117.

Poskanzer, K., Needleman, L.A., Bozdagi, O., Huntley, G.W., 2003. N-cadherin regulates ingrowth and laminar targeting of thalamocortical axons. J. Neurosci. 23, 2294–2305.

Prakash, S., Caldwell, J.C., Eberl, D.F., Clandinin, T.R., 2005. *Drosophila* N-cadherin mediates an attractive interaction between photoreceptor axons and their targets. Nat. Neurosci. 8, 443–450.

Prakash, S., McLendon, H.M., Dubreuil, C.I., Ghose, A., Hwa, J., Dennehy, K.A., Tomalty, K.M., Clark, K.L., Van Vactor, D., Clandinin, T.R., 2009. Complex interactions amongst N-cadherin, DLAR, and Liprin-alpha regulate *Drosophila* photoreceptor axon targeting. Dev. Biol. 336, 10–19.

Pulver, S.R., Pashkovski, S.L., Hornstein, N.J., Garrity, P.A., Griffith, L.C., 2009. Temporal dynamics of neuronal activation by Channelrhodopsin-2 and TRPA1 determine behavioral output in *Drosophila* larvae. J. Neurophysiol. 101, 3075–3088.

Rohrbough, J., O'Dowd, D.K., Baines, R.A., Broadie, K., 2003. Cellular bases of behavioral plasticity: establishing and modifying synaptic circuits in the *Drosophila* genetic system. J. Neurobiol. 54, 254–271.

Saglietti, L., Dequidt, C., Kamieniarz, K., Rousset, M.C., Valnegri, P., Thoumine, O., Beretta, F., Fagni, L., Choquet, D., Sala, C., Sheng, M., Passafaro, M., 2007. Extracellular interactions between GluR2 and N-cadherin in spine regulation. Neuron 54, 461–477.

Spitzer, N.C., 2002. Activity-dependent neuronal differentiation prior to synapse formation: the functions of calcium transients. J. Physiol. 96, 73–80.

Spitzer, N.C., 2006. Electrical activity in early neuronal development. Nature 444, 707–712.

Suzuki, S.C., Takeichi, M., 2008. Cadherins in neuronal morphogenesis and function. Dev. Growth Differ. 50 (Suppl. 1), S119–130.

Tang, L., Hung, C.P., Schuman, E.M., 1998. A role for the cadherin family of cell adhesion molecules in hippocampal long-term potentiation. Neuron 20, 1165–1175.

Ting, C.Y., Yonekura, S., Chung, P., Hsu, S.N., Robertson, H.M., Chiba, A., Lee, C.H., 2005. *Drosophila* N-cadherin functions in the first stage of the two-stage layer-selection process of R7 photoreceptor afferents. Development 132, 953–963.

Togashi, H., Abe, K., Mizoguchi, A., Takaoka, K., Chisaka, O., Takeichi, M., 2002. Cadherin regulates dendritic spine morphogenesis. Neuron 35, 77–89.

Uchida, N., Honjo, Y., Johnson, K.R., Wheelock, M.J., Takeichi, M., 1996. The catenin/cadherin adhesion system is localized in synaptic junctions bordering transmitter release zones. J. Cell Biol. 135, 767–779.

Wang, J., Ma, X., Yang, J.S., Zheng, X., Zugates, C.T., Lee, C.H., Lee, T., 2004. Transmembrane/juxtamembrane domain-dependent Dscam distribution and function during mushroom body neuronal morphogenesis. Neuron 43, 663–672.

Yamagata, M., Herman, J.P., Sanes, J.R., 1995. Lamina-specific expression of adhesion molecules in developing chick optic tectum. J. Neurosci. 15, 4556–4571.

Yasuyama, K., Meinertzhagen, I.A., Schurmann, F.W., 2002. Synaptic organization of the mushroom body calyx in *Drosophila melanogaster*. J. Comp. Neurol. 445, 211–226.

Yonekura, S., Ting, C.Y., Neves, G., Hung, K., Hsu, S.N., Chiba, A., Chess, A., Lee, C.H., 2006. The variable transmembrane domain of *Drosophila* N-cadherin regulates adhesive activity. Mol. Cell. Biol. 26, 6598–6608.

Zhan, X.L., Clemens, J.C., Neves, G., Hattori, D., Flanagan, J.J., Hummel, T., Vasconcelos, M.L., Chess, A., Zipursky, S.L., 2004. Analysis of Dscam diversity in regulating axon guidance in *Drosophila* mushroom bodies. Neuron 43, 673–686.

Zhu, H., Luo, L., 2004. Diverse functions of N-cadherin in dendritic and axonal terminal arborization of olfactory projection neurons. Neuron 42, 63–75.